

# Stabilization of ion temperature gradient driven modes by lower hybrid wave in a tokamak

Animesh Kuley<sup>a)</sup> and V. K. Tripathi

Department of Physics, Indian Institute of Technology Delhi, New Delhi-110016, India

(Received 2 September 2008; accepted 22 January 2009; published online 11 March 2009)

A gyrokinetic formalism has been developed to study lower hybrid wave stabilization of ion temperature gradient driven modes, responsible for anomalous ion transport in the inner region of tokamak. The parametric coupling between lower hybrid and drift waves produce lower hybrid sideband waves. The pump and the sidebands exert a ponderomotive force on electrons, modifying the eigenfrequency of the drift wave and influencing the growth rate. The longer wavelength drift waves are destabilized by the lower hybrid wave while the shorter wavelengths are suppressed. The requisite lower hybrid power is in the range of  $\sim 900$  kW at 4.6 GHz. © 2009 American Institute of Physics. [DOI: 10.1063/1.3080744]

## I. INTRODUCTION

Microinstabilities in magnetically confined plasma have been studied extensively as a key mechanism for producing plasma turbulence and resultant anomalous transport.<sup>1-9</sup> Three types of drift waves, viz., ion temperature gradient (ITG) mode,<sup>1,10</sup> trapped electron mode,<sup>1,10,11</sup> and electron temperature gradient (ETG) mode driven by passing electrons<sup>12-15</sup> are believed to affect plasma confinement. The ITG mode is essentially an electrostatic instability, driven by the free energy contained in ion temperature gradient. It is more unstable for lower beta plasmas. In toroidal geometry, the modes are also driven by the unfavorable magnetic curvature, although the mode may remain essentially slablike in the region of weak/negative shear.<sup>16,17</sup>

Redi *et al.*<sup>9</sup> analyzed linear drift mode stability in Alcator C-Mod with radio frequency heating, using GS2 gyrokinetic code, and shown that ITG and ETG modes are unstable outside the barrier region and not strongly growing in the core; in the barrier region ITG is only weakly unstable. Applegate *et al.*<sup>8</sup> showed that electrostatic ITG modes can be stabilized if the ion pressure gradient can be supported by the ion density profile instead of the ion temperature profile in mega-ampere spherical tokamak like plasma by using GS2 code. Fivaz *et al.*,<sup>18</sup> showed that ITG modes can be stabilized by a reduction of the equilibrium  $\nabla \mathbf{B}$  drifts by using global gyrokinetic particle simulation. Falchetto and Ottaviani<sup>19</sup> showed an increase in energy confinement time and a stabilization of ITG driven turbulence with the inverse of collisionality of zonal flows by three-dimensional (3D) global fluid model. Watanabe *et al.*<sup>20</sup> numerically showed that helical configuration optimized for reducing neoclassical ripple transport can simultaneously reduce turbulent transport with enhancing zonal-flow generation by gyrokinetic Vlasov simulation. Lin *et al.*<sup>21</sup> showed that nonlinear global simulation of instabilities driven by temperature gradients in ion component of the plasma support the view that turbulence driven fluctuating zonal flows can substantially reduce turbu-

lent transport by 3D global gyrokinetic toroidal code. Jhowry and Anderson<sup>22</sup> investigated the stability of electromagnetic ion temperature gradient driven modes by finite beta ( $\beta$ ) in noncircular toroidal devices.

In this paper we develop a gyro kinetic formalism to study the effect of high power lower hybrid wave on electrostatic ITG driven modes in advanced tokamak. Lower hybrid waves are launched into a tokamak by a phased array of waveguides. As they propagate toward the center in a well defined resonance cone they attain larger amplitude at higher densities and become susceptible to parametric instabilities.<sup>23</sup> In the presence of lower hybrid pump wave ( $\omega_0, \mathbf{k}_0$ ), the electrons acquire an oscillatory velocity,  $\mathbf{v}_0$ . When this is combined with a lower frequency density perturbation, a nonlinear current is produced which is the source to drive lower hybrid resonant waves at sideband frequencies ( $\omega_1, \omega_2$ ). These sidebands beat with the pump to produce a ponderomotive force, driving or suppressing the low frequency perturbation.

In Sec. II we obtain the linear response of electrons to the pump and sideband waves. Nonlinear low frequency response has been studied in Sec. III. Section IV contains the nonlinear response at sidebands, and growth rate have been calculated in Sec. V. Conclusions have been given in Sec. VI.

## II. LINEAR RESPONSE OF THE PUMP AND SIDEBANDS

We model the tokamak by a plasma slab of nonuniform electron density  $n_0(x)$  and temperature  $T_0(x)$  in shearless magnetic field  $\mathbf{B} = B_0 \hat{z}$ . The  $x$ ,  $y$ , and  $z$  directions in the slab geometry correspond to radial, poloidal, and toroidal directions in the tokamak configuration. A high power lower hybrid wave is launched into the plasma with potential  $\phi_0 = \phi_0 e^{-i(\omega_0 t - \mathbf{k}_{0\perp} \cdot \mathbf{r} - k_{0z} z)}$ . This wave imparts oscillatory velocity to electrons,

$$\mathbf{v}_{0\perp} = \frac{e}{m\omega_c^2} [\omega_c \times \nabla_{\perp} \phi_0 - i\omega_0 \nabla_{\perp} \phi_0],$$

<sup>a)</sup>Electronic mail: animesh.kuley@mail2.iitd.ac.in.

$$v_{0z} = -\frac{ek_{0z}}{m\omega_0} \phi_0, \quad (1)$$

where  $\omega_0$  lies in the range  $\omega_{ci} \ll \omega_0 \ll \omega_c$ ,  $\omega_0 = \omega_{pi} [1 + (k_{0z}^2 m_i / k_0^2 m)]^{1/2} [1 + (\omega_p^2 / \omega_c^2)]^{-1/2}$ ,  $\omega_c = eB_0/m$ ,  $\omega_p = (n_0 e^2 / m \epsilon_0)^{1/2}$ ,  $\omega_{pi} = (n_0 e^2 / m_i \epsilon_0)^{1/2}$ ,  $-e$ , and  $m$  be the charge, and mass of the electron, and  $m_i$  be the mass of the ion. The first term on the right hand side of Eq. (1) is the  $\mathbf{E}_0 \times \mathbf{B}$  drift which is much larger than the polarization drift (the second term in the same equation) and the parallel velocity. This oscillatory velocity provides a coupling between a ion temperature gradient drift mode of potential

$$\phi = A e^{-i(\omega t - \mathbf{k} \cdot \mathbf{r})} \quad (2)$$

and lower hybrid wave sidebands of potential

$$\phi_j = A_j e^{-i(\omega_j t - \mathbf{k}_j \cdot \mathbf{r})} \quad (3)$$

with  $j=1,2$  where  $\omega_1 = \omega - \omega_0$ ,  $\omega_2 = \omega + \omega_0$ ,  $\mathbf{k}_1 = \mathbf{k} - \mathbf{k}_0$ , and  $\mathbf{k}_2 = \mathbf{k} + \mathbf{k}_0$ . The linear response of the electron for two sidebands turns out to be

$$\mathbf{v}_{j\perp} = \frac{e}{m\omega_c^2} [\omega_c \times \nabla_{\perp} \phi_j - i\omega_j \nabla_{\perp} \phi_j], \quad (4)$$

$$v_{jz} = -\frac{ek_{jz}}{m\omega_j} \phi_j.$$

### III. NONLINEAR LOW FREQUENCY RESPONSE

The sidebands couple with the lower hybrid pump to produce a low frequency ponderomotive force  $\mathbf{F}_p$  on the electrons.  $\mathbf{F}_p$  has two components, perpendicular and parallel to the magnetic field. The response of electrons to  $\mathbf{F}_p$  is strongly suppressed by the magnetic field and is usually weak. In the parallel direction, the electrons can effectively respond to  $\mathbf{F}_{pz}$ , hence, the low frequency nonlinearity arises mainly through  $\mathbf{F}_{pz} = -m\mathbf{v} \cdot \nabla v_z$ . The parallel ponderomotive force, using the complex number identity  $ReA \times ReB = (1/2)Re[A \times B + A^* \times B]$ , can be written as

$$\mathbf{F}_{pz} = eik_z \phi_p = -\left(\frac{m}{2}\right) [\mathbf{v}_{0\perp} \cdot \nabla_{\perp} v_{1z} + \mathbf{v}_{1\perp} \cdot \nabla_{\perp} v_{0z}] - \left(\frac{m}{2}\right) [\mathbf{v}_{0\perp}^* \cdot \nabla_{\perp} v_{2z} + \mathbf{v}_{2\perp} \cdot \nabla_{\perp} v_{0z}^*]. \quad (5)$$

Using Eqs. (1) and (4) and considering only the dominant  $\mathbf{E}_0 \times \mathbf{B}$  drift terms the ponderomotive potential  $\phi_p$  in the limit  $\omega \ll k_z v_{the}$ , takes the form

$$\phi_p = \frac{e\phi_0\phi_1}{2m\omega_c^2} \frac{\mathbf{k}_{1\perp} \cdot \mathbf{k}_{0\perp} \times \omega_c}{ik_z \omega_0 \omega_1} (\omega_0 k_{1z} - \omega_1 k_{0z}) + \frac{e\phi_0^* \phi_2}{2m\omega_c^2} \frac{\mathbf{k}_{2\perp} \cdot \mathbf{k}_{0\perp} \times \omega_c}{ik_z \omega_0 \omega_2} (\omega_0 k_{2z} - \omega_2 k_{0z}), \quad (6)$$

where  $v_{the} = (2T_e/m)^{1/2}$  is the electron thermal velocity. One may note  $\phi_p$  is maximum when  $\mathbf{k}_{\perp}$  and  $\mathbf{k}_{0\perp}$  are perpendicular to each other. The response electrons to ponderomotive potential  $\phi_p$  and the self consistent potential  $\phi$  is governed by the Vlasov equation

$$\frac{\partial}{\partial t} f + \mathbf{v} \cdot \nabla f + \frac{e}{m} [\nabla(\phi + \phi_p) - \mathbf{v} \times \mathbf{B}] \cdot \nabla_{\mathbf{v}} f = 0. \quad (7)$$

We consider the equilibrium distribution function with non-uniform density and temperature as

$$f_0 = n_0^0 \left[ 1 - \frac{x - \frac{v_y}{\omega_c}}{L_n} \right] \times \left[ \frac{m}{2\pi T_0 \left( 1 - \frac{x - \frac{v_y}{\omega_c}}{L_T} \right)} \right]^{3/2} \exp \left[ -\frac{mv^2}{2T_0 \left( 1 - \frac{x - \frac{v_y}{\omega_c}}{L_T} \right)} \right], \quad (8)$$

where  $L_n$  and  $L_T$  are the density and temperature scale lengths. Perturbing this equilibrium by  $f = f_0 + f_1$  and linearizing we obtain

$$f_1 = -\frac{e}{m} \int_{-\infty}^t \left[ \nabla(\phi + \phi_p) \cdot \left( \frac{\partial}{\partial \mathbf{v}} f_0 \right) \right]_{t'} dt', \quad (9)$$

where the integration is over the unperturb trajectory. Equation (9) simplifies to give

$$f_1 = \frac{n_0^0 e (\phi + \phi_p)}{m} \left( \frac{m}{2\pi T_0} \right)^{3/2} e^{-mv^2/2T_0} \sum_l \sum_n J_l \left( \frac{k_{\perp} v_{\perp}}{\omega_c} \right) J_n \left( \frac{k_{\perp} v_{\perp}}{\omega_c} \right) \frac{1}{\omega - l\omega_c - k_z v_z} e^{i(l-n)\theta} \left[ \frac{k_y}{\omega_c} \left( \frac{1}{L_n} - \frac{1}{L_T} \left( \frac{3}{2} - \frac{mv^2}{2T_0} \right) \right) - \left[ 1 - \left( x - \frac{v_y}{\omega_c} \right) \left( \frac{1}{L_n} - \frac{1}{L_T} \left( \frac{5}{2} - \frac{mv^2}{2T_0} \right) \right) \right] (l\omega_c + k_z v_z) \right], \quad (10)$$

where  $J_l$  and  $J_n$  are the Bessel functions of order  $l$  and  $n$ , and  $\theta$  is the gyrophase angle. The perturbed density of electrons turns out to be

$$n = \int_0^{\infty} \int_0^{2\pi} \int_{-\infty}^{\infty} f_1 v_{\perp} dv_{\perp} d\theta dv_z, \quad (11)$$

$$\begin{aligned}
n = & (\phi + \phi_p) \left[ \frac{2n_0^0 e}{mv_{th}^2} \left( 1 + \frac{\omega - \omega_n^* + \frac{3}{2}\omega_T^*}{k_z v_{th}} \sum_l Z(\xi) I_l e^{-b} + \frac{v_{th}}{\omega_c L_T} \sum_l \frac{l}{2\beta} \frac{I_l e^{-b}}{2} \right) + \frac{n_0^0 e}{mv_{th}^2} \sum_l \left[ \left( \frac{v_{th}}{\omega_c L_n} - \frac{5}{2} \frac{v_{th}}{\omega_c L_T} \right) I_l e^{-b} \right. \right. \\
& \left. \left. + \frac{2v_{th}}{\omega_c L_T} \frac{\partial}{\partial b} (b I_l e^{-b}) \right) \right] \left[ 1 + \frac{\omega}{k_z v_{th}} Z(\xi) \right] - \frac{2n_0^0 e}{mv_{th}^2} \sum_l \left[ \frac{\omega_T^*}{k_z v_{th}} I_l e^{-b} - \frac{v_{th}}{\omega_c L_T k_z v_{th}} \left( \frac{l}{2\beta} I_l e^{-b} - \frac{b^{1/2}}{4} \frac{\partial}{\partial b} (I_l e^{-b}) \right) \right] [\xi + \xi^2 Z(\xi)] \\
& - \frac{n_0^0 e}{mv_{th}^2} \sum_l \left[ \left( \frac{v_{th}}{\omega_c L_n} - \frac{5}{2} \frac{v_{th}}{\omega_c L_T} \right) \frac{b^{1/2}}{2} \frac{\partial}{\partial b} (I_l e^{-b}) \frac{\omega}{k_z v_{th}} + \frac{\omega_T^*}{k_z v_{th}} \frac{\partial}{\partial b} (b I_l e^{-b}) + \frac{v_{th}}{\omega_c L_T} \frac{1}{4b^{1/2}} \frac{\partial}{\partial b} \left( b^2 \frac{\partial}{\partial b} (I_l e^{-b}) \right) \frac{\omega}{k_z v_{th}} \right] Z(\xi) \Big], \quad (12)
\end{aligned}$$

where  $\omega_T^* = k_y T_0 / m \omega_c L_T$ , and  $\omega_n^* = k_y T_0 / m \omega_c L_n$  are the diamagnetic drift frequencies,  $\xi = (\omega - l \omega_c / k_z v_{th})$ ,  $I_n(b)$  is the modified Bessel function of order  $n$  and argument  $b$ ,  $Z(\xi)$  is the plasma dispersion function, and we have used the identity

$$\int_0^\infty e^{-s^2} J_n^2(\alpha s) s ds = \frac{1}{2} I_n e^{-b}, \quad (13)$$

$$\int_0^\infty e^{-s^2} J_n'(\alpha s) J_n(\alpha s) s^2 ds = \frac{b^{1/2}}{4} \frac{d}{db} (I_n e^{-b}).$$

For the ITG mode of  $\omega \ll \omega_{ci}$ ,  $n$  simplifies to

$$n = \frac{k^2}{e} \epsilon_0 \chi_e (\phi + \phi_p), \quad (14)$$

$$\begin{aligned}
\chi_e = \chi_{er} + i\chi_{ei} = & \frac{2\omega_p^2}{k^2 v_{the}^2} \left[ 1 + \frac{\omega - \omega_n^* + \frac{3}{2}\omega_T^*}{k_z v_{the}} Z\left(\frac{\omega}{k_z v_{the}}\right) \right] \\
& - \frac{2\omega_p^2}{k^2 v_{the}^2} \frac{\omega_T^*}{k_z v_{the}} \left[ Z\left(\frac{\omega}{k_z v_{the}}\right) + \frac{\omega}{k_z v_{the}} \right]. \quad (15)
\end{aligned}$$

In the limit  $\omega \ll k_z v_{the}$  one can write

$$\begin{aligned}
\chi_{er} = & 2 \frac{\omega_p^2}{k^2 v_{the}^2} \left[ 1 - \frac{\omega - \omega_n^* + \frac{3}{2}\omega_T^*}{k_z v_{the}} \left( \frac{\omega}{k_z v_{the}} \right) \right], \\
\chi_{ei} = & 2 \frac{\omega_p^2}{k^2 v_{the}^2} \sqrt{\pi} \left[ \frac{\omega - \omega_n^* + \frac{1}{2}\omega_T^*}{k_z v_{the}} \right]. \quad (16)
\end{aligned}$$

Ion density perturbation can be recovered from  $n$  by replacing  $\omega_c$  by  $\omega_{ci}$  ( $\omega_{ci} = eB_0/m_i$  where  $m_i$  is the ion mass and  $e$  is the ion charge),  $v_{th}$  by  $v_{thi}$ ,  $\omega_n^*$  by  $-\omega_{ni}^*$ ,  $\omega_T^*$  by  $-\omega_{Ti}^*$ ,  $e$ ,  $T_e$  by  $-e$ ,  $T_i$  and ignoring  $\phi_p$ .

In the limit of  $\omega \gg k_z v_{thi}$  one may write

$$n_i = -\frac{k^2}{e} \epsilon_0 (\chi_{ir} + i\chi_{ii}) \phi, \quad (17)$$

$$\begin{aligned}
\chi_{ir} = & 2 \frac{\omega_{pi}^2}{k^2 v_{thi}^2} \left[ \frac{(\omega_{ni}^* - \frac{3}{2}\omega_{Ti}^*)(1 - b_i) + \omega_{Ti}^*(1 - 2b_i)}{\omega} \right. \\
& \left. - \left( \frac{v_{thi}}{4\omega_{ci} L_{ni}} - \frac{v_{thi}}{8\omega_{ci} L_{Ti}} \right) b_i^{1/2} \right],
\end{aligned}$$

$$\begin{aligned}
\chi_{ii} = & 2 \frac{\omega_{pi}^2}{k^2 v_{thi}^2} \sqrt{\pi} \left[ \frac{\omega_{ni}^* - \frac{3}{2}\omega_{Ti}^*}{k_z v_{thi}} (1 - b_i) + \frac{\omega_{Ti}^*}{k_z v_{thi}} (1 - 2b_i) \right. \\
& \left. + \left[ \frac{\omega}{k_z v_{thi}} (1 - b_i) + \left( \frac{v_{thi}}{4\omega_{ci} L_{ni}} \right. \right. \right. \\
& \left. \left. \left. - \frac{v_{thi}}{8\omega_{ci} L_{Ti}} \right) b_i^{1/2} \right] \right] e^{-\omega^2/k_z^2 v_{thi}^2}. \quad (18)
\end{aligned}$$

Now using the Eqs. (14) and (17) in the Poisson equation  $\nabla^2 \phi = (e/\epsilon_0)(n - n_i)$  we obtain

$$\varepsilon \phi = -\chi_e \phi_p, \quad (19)$$

where  $\varepsilon = 1 + \chi_i + \chi_e$ .

#### IV. NONLINEAR RESPONSE AT THE SIDEBANDS

The density perturbation at  $(\omega, \mathbf{k})$  couples with the oscillatory velocity of electrons,  $\mathbf{v}_0$ , to produce nonlinear density perturbations at sideband frequencies. Solving the equation of continuity,

$$\frac{\partial}{\partial t} n_1^{\text{NL}} + \nabla \cdot \left( \frac{n}{2} v_0^* \right) = 0, \quad (20)$$

one obtains

$$n_1^{\text{NL}} = \frac{n}{2\omega_1} (\mathbf{k}_1 \cdot \mathbf{v}_0^*). \quad (21)$$

similarly for the upper sideband the nonlinear density perturbation can be written as

$$n_2^{\text{NL}} = \frac{n}{2\omega_2} (\mathbf{k}_2 \cdot \mathbf{v}_0^*). \quad (22)$$

Using Eqs. (21) and (22) in Poisson's equation for the sideband waves, we obtain

$$\begin{aligned}
\varepsilon_1 \phi_1 = & \frac{k^2}{k_1^2} (1 + \chi_i) \frac{\mathbf{k}_1 \cdot \mathbf{v}_0^*}{2\omega_1} \phi, \\
\varepsilon_2 \phi_2 = & \frac{k^2}{k_2^2} (1 + \chi_i) \frac{\mathbf{k}_2 \cdot \mathbf{v}_0}{2\omega_2} \phi, \quad (23)
\end{aligned}$$

where

$$\varepsilon_1 = 1 + \frac{\omega_p^2}{\omega_c^2} - \frac{\omega_{pi}^2}{\omega_1^2} \left( 1 + \frac{k_{1z}^2 m_i}{k_1^2 m} \right),$$

$$\varepsilon_2 = 1 + \frac{\omega_p^2}{\omega_c^2} - \frac{\omega_{pi}^2}{\omega_0^2} \left( 1 + \frac{k_z^2 m_i}{k_\perp^2 m} \right), \quad (24)$$

are the dielectric functions at  $(\omega_1, \mathbf{k}_1)$ , and  $(\omega_2, \mathbf{k}_2)$ .

## V. GROWTH RATE

The nonlinear coupled Eqs. (19) and (23) lead to the nonlinear dispersion relation

$$\varepsilon = \mu \left[ \frac{1}{\varepsilon_1} + \frac{1}{\varepsilon_2} \right], \quad (25)$$

where

$$\mu = - \frac{\chi_e(1 + \chi_i) k^2 U^2 \sin^2 \delta}{\left( 1 + \frac{k_{0\perp}^2}{k_\perp^2} \right) 4\omega_0^2}, \quad (26)$$

$U = ek_0 \phi_0 / m\omega_c$  is the magnitude of  $\mathbf{E}_0 \times \mathbf{B}$  electron velocity, and  $\delta$  is the angle between  $\mathbf{k}_\perp$  and  $\mathbf{k}_{0\perp}$ . For  $\omega k_{0z} / \omega_0 k_z \ll 1$ , one may write

$$\varepsilon_1 = \alpha_1 + \beta\omega, \quad (27)$$

$$\varepsilon_2 = \alpha_2 - \beta\omega,$$

where

$$\begin{aligned} \alpha_1 &= \left( 1 + \frac{\omega_p^2}{\omega_c^2} \right) - \frac{\omega_{pi}^2}{\omega_0^2} \left( 1 + \frac{m_i(k_z + k_{0z})^2}{m k_{0\perp}^2 + k_\perp^2} \right) \\ &\simeq \left( 1 + \frac{\omega_p^2}{\omega_c^2} \right) \left( 1 - \frac{\omega_{LH}^2}{\omega_0^2} \right) \left( \frac{k_\perp^2}{k_{0\perp}^2} - 2 \frac{k_z}{k_{0z}} \right), \end{aligned}$$

$$\begin{aligned} \alpha_2 &= \left( 1 + \frac{\omega_p^2}{\omega_c^2} \right) - \frac{\omega_{pi}^2}{\omega_0^2} \left( 1 + \frac{m_i(k_z - k_{0z})^2}{m k_{0\perp}^2 + k_\perp^2} \right) \\ &\simeq \left( 1 + \frac{\omega_p^2}{\omega_c^2} \right) \left( 1 - \frac{\omega_{LH}^2}{\omega_0^2} \right) \left( \frac{k_\perp^2}{k_{0\perp}^2} + 2 \frac{k_z}{k_{0z}} \right), \end{aligned}$$

$$\beta = \frac{2}{\omega_0} \left( 1 + \frac{\omega_p^2}{\omega_c^2} \right). \quad (28)$$

Now using Eqs. (16), (18), and (25) the nonlinear dispersion relation can be written as

$$\begin{aligned} (1 + \chi_{ir} + \chi_{er})[\alpha_1 \alpha_2 + (\alpha_2 - \alpha_1)\beta\omega] + P(\chi_{er} + \chi_{er}\chi_{ir}) \\ + i(\chi_{ii} + \chi_{ei})[\alpha_1 \alpha_2 + (\alpha_2 - \alpha_1)\beta\omega] + P(\chi_{ei} + \chi_{ii}\chi_{er} \\ + \chi_{ei}\chi_{ir}) = 0, \end{aligned} \quad (29)$$

where

$$P = \frac{U^2 k^2}{4\omega_0^2} \left( \frac{1}{1 + \frac{k_{0\perp}^2}{k_\perp^2}} \right) (\alpha_1 + \alpha_2). \quad (30)$$

Writing  $\omega = \omega_r + i\gamma$ , with  $\gamma \ll \omega_r$ , the real and imaginary parts of Eq. (29) gives

$$\omega_r = - \frac{G \left[ P + \alpha_1 \alpha_2 \frac{k^2 v_{the}^2}{2\omega_p^2} \right]}{\frac{k^2 v_{the}^2}{2\omega_p^2} [G\beta(\alpha_2 - \alpha_1) + H] - PG \frac{\frac{3}{2}\omega_r^* - \omega_n^*}{k_z^2 v_{the}^2}}, \quad (31)$$

where

$$G = 2 \frac{\omega_{pi}^2}{k^2 v_{thi}^2} \left[ \left( \omega_{ni}^* - \frac{3}{2} \omega_{Ti}^* \right) (1 - b_i) + \omega_{Ti}^* (1 - 2b_i) \right],$$

$$H = \alpha_1 \alpha_2 \left( 1 + 2 \frac{\omega_p^2}{k^2 v_{the}^2} - 2 \frac{\omega_{pi}^2}{k^2 v_{thi}^2} \left( \frac{v_{thi}}{4\omega_{ci} L_{ni}} - \frac{1}{8} \frac{v_{thi}}{\omega_{ci} L_{Ti}} \right) \right) + 2P \frac{\omega_p^2}{k^2 v_{the}^2} \left( 1 - 2 \frac{\omega_{pi}^2}{k^2 v_{thi}^2} \left( \frac{v_{thi}}{4\omega_{ci} L_{ni}} - \frac{1}{8} \frac{v_{thi}}{\omega_{ci} L_{Ti}} \right) \right). \quad (32)$$

In the absence of lower hybrid power ( $P=0$ ) the above expression simplifies to

$$\omega_r = - \frac{G}{G\beta \left( \frac{1}{\alpha_1} - \frac{1}{\alpha_2} \right) + \left[ 1 + 2 \frac{\omega_p^2}{k^2 v_{the}^2} - \frac{\omega_{pi}^2}{k^2 v_{thi}^2} \frac{v_{thi}}{2\omega_{ci}} \left( \frac{1}{L_{ni}} - \frac{1}{2L_{Ti}} \right) \right]}, \quad (33)$$

$$\begin{aligned} \gamma = - \frac{\left[ (\chi_{ii} + \chi_{ei}) \left[ 1 + \left( \frac{1}{\alpha_1} - \frac{1}{\alpha_2} \right) \beta\omega \right] \right]_{\omega=\omega_r}}{\frac{\partial}{\partial \omega} \left[ (1 + \chi_{ir} + \chi_{er}) \left[ 1 + \left( \frac{1}{\alpha_1} - \frac{1}{\alpha_2} \right) \beta\omega \right] \right]_{\omega=\omega_r}}. \end{aligned} \quad (34)$$

In order to have a numerical appreciation of results we consider the following set of parameters, corresponding to Alcator C-Mod:<sup>24</sup> electron density  $1 \times 10^{20} \text{ m}^{-3}$ , magnetic field  $\approx 5 \text{ T}$ , and source frequency of 4.6 GHz with  $k_{0\parallel} c / \omega_0 \approx 2$ ,  $T_i \approx T_e \approx 1 \text{ keV}$ , for  $U/c_s = 3$ , where  $c_s$  is the ion sound speed. The value of  $U/c_s = 3$  corresponds to lower hybrid power of 1.7 MW.<sup>25</sup> One may mention that the range of lower hybrid power is typically  $\sim 1 \text{ MW}$  and looking for the

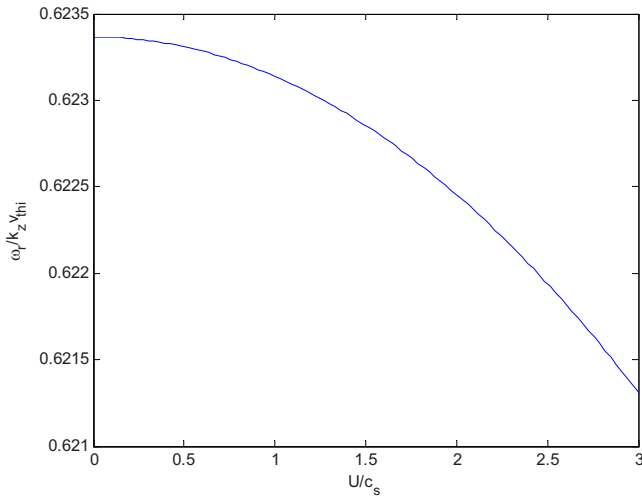


FIG. 1. (Color online) Progression of dispersion relation curve as a function of normalized LH-mode amplitude for  $\eta_i=4$ .

increase in LH power to 2.0–2.4 MW in future. Figure 1 shows the progression of normalized wave frequency for electrostatic ITG mode as a function of the lower hybrid pump power which shows only tiny decrease in lower hybrid amplitude i.e., the effect of LH pump wave on real frequency is negligible, while the lower hybrid pump amplitude have a significant effect on growth rate (cf. Fig. 2). Electrostatic ITG modes have positive real frequencies since they propagate in the ion diamagnetic direction as observed by Applegate *et al.*<sup>8</sup> Figures 3 and 4 show modest downshift in wave number in the normalized growth rate as a function of normalized wave number, and the growth rate is increased for  $k_{\perp}\rho_i < 0.17$  in Fig. 3 and for  $k_{\perp}\rho_i < 0.1$  in Fig. 4. (The spectra in nonlinear ITG simulations tend to peak at wave numbers much lower than the peak growth rate, this wave number downshift of the curves may actually result in an increase in the transport rates). [cf. Fig. 5, Redi *et al.*<sup>9</sup>] and [cf. Fig. 8, Applegate *et al.*<sup>8</sup>] show instability growth rates calculated with linear dispersion codes using experimental profiles

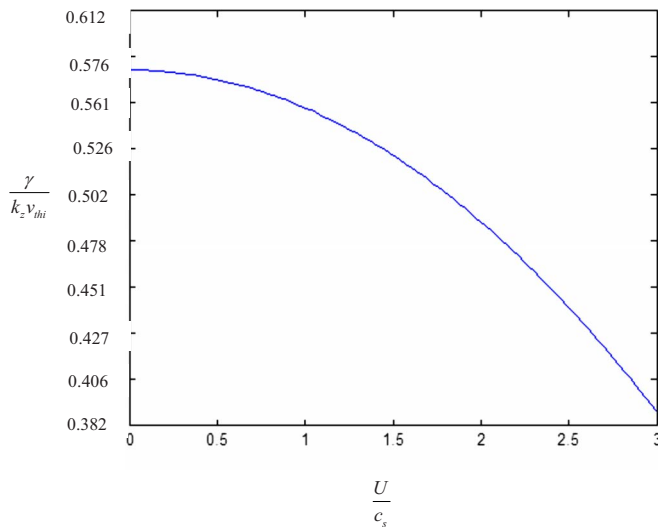


FIG. 2. (Color online) Growth rate as a function of normalized LH-mode amplitude for  $\eta_i=4$ .

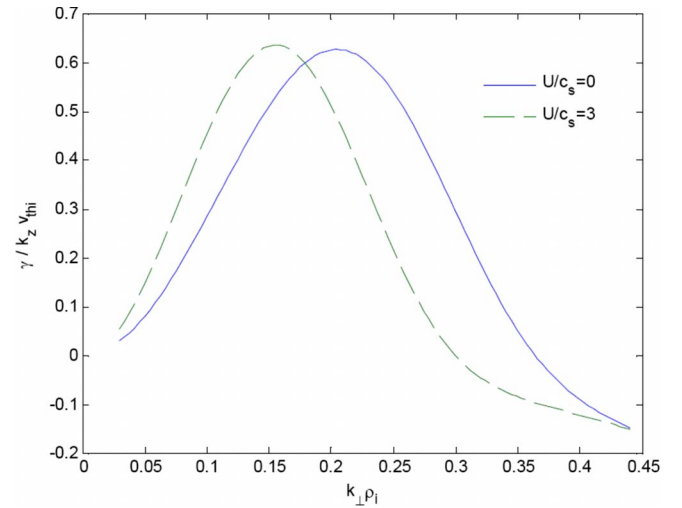


FIG. 3. (Color online) Variation of normalized growth rate of ITG mode drift wave as a function of normalized wave vector for  $U/c_s=0$  and 3 with  $\eta_i=3$ .

which have been modified by ion cyclotron radio frequency heating. Those calculations do not contain a ponderomotive stabilization mechanism of the type addressed in this paper.

## VI. CONCLUSION

At lower hybrid power level of  $\sim 1$  MW at  $\omega_0 \lesssim 2\omega_{LH}$  and  $k_{0z} \sim (1.5-2)\omega_0/c$ , the ion temperature gradient driven mode is strongly affected by the nonlinear coupling. For typical tokamak parameters<sup>24</sup> the growth rate is significantly affected by the lower hybrid pump i.e., the short wavelength are suppressed while the others are destabilized by the lower hybrid wave and with the increasing of  $\eta_i$  longer wavelength drift modes are more unstable, for the regime where  $k_z v_{thi}$  is comparable with  $\omega^*$ . This paper actually appears to show is that the lower hybrid (LH) pump is likely to have a significant on transport driven by ITG modes. From Eq. (31) it has been observed that the stabilization of the drift wave are

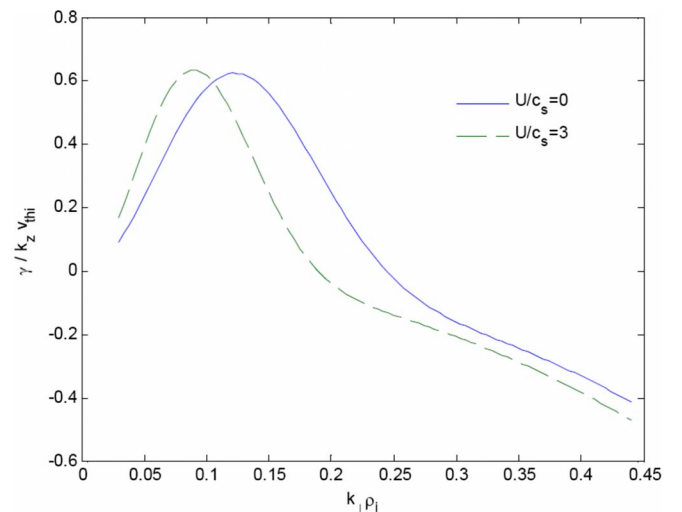


FIG. 4. (Color online) Variation of normalized growth rate of ITG mode drift wave as a function of normalized wave vector for  $U/c_s=0$  and 3 with  $\eta_i=5$ .

effective when  $P \sim \alpha_1 \alpha_2 (k^2 v_{\text{the}}^2 / 2 \omega_p^2)$  or above. It may be noted that the drift wave in a tokamak are greatly affected by the magnetic shear and toroidal effects and the analysis of present paper may not be applicable as such.

## ACKNOWLEDGMENTS

The authors would like to thank Professor J. W. Connor of UKAEA Culham, Dr. W. A. Houlberg of the Oak Ridge National Laboratory, USA, Professor D. J. Campbell of the Fusion Science and Technology Department, ITER Organization, CEA Cadarache Centre, France, Professor Nikhil Chakrabarti, and Professor Rabindra Nath Pal of Plasma Physics Division, Saha Institute of Nuclear Physics for their assistance.

<sup>1</sup>W. Horton, *Rev. Mod. Phys.* **71**, 735 (1999).

<sup>2</sup>T. Yamada, S. Itoh, T. Maruta, N. Kasuya, Y. Nagashima, S. Shinohara, K. Terasaka, M. Yagi, S. Inagaki, Y. Kawai, A. Fujisawa, and K. Itoh, *Nat. Phys.* **4**, 721 (2008).

<sup>3</sup>A. M. Dimits, G. Bateman, M. A. Beer, B. I. Cohen, W. Dorland, G. W. Hammett, C. Kim, J. E. Kinsey, M. Kotschenreuther, A. H. Kritiz, L. L. Lao, J. Mandrekas, W. M. Nevins, S. E. Parker, A. J. Redd, D. E. Shumaker, R. Sydora, and J. Weiland, *Phys. Plasmas* **7**, 969 (2000).

<sup>4</sup>F. Jenko, W. Dorland, M. Kotschenreuther, and B. N. Rogers, *Phys. Plasmas* **7**, 1904 (2000).

<sup>5</sup>J. W. Connor and H. R. Wilson, *Plasma Phys. Controlled Fusion* **36**, 719 (1994).

<sup>6</sup>E. J. Doyle, W. A. Houlberg, Y. Kamada, V. Mukhovatov, T. H. Osborne, A. Polevoi, G. Bateman, J. W. Connor, J. G. Cordey, T. Fujita, X. Garbet, T. S. Hahm, L. D. Horton, A. E. Hubbard, F. Imbeaux, F. Jenko, J. E. Kinsey, Y. Kishimoto, J. Li, T. C. Luce, Y. Martin, M. Ossipenko, V. Parail, A. Peeters, T. L. Rhodes, J. E. Rice, C. M. Roach, V. Rozhansky, F. Ryter, G. Saibene, R. Sartori, A. C. C. Sips, J. A. Snipes, M. Sughira, E. J. Synakowski, H. Takenaga, T. Takizuka, K. Thomsen, M. R. Wade, H. R. Wilson, ITPA Transport Physics Topical Group, ITPA Confinement Database and Modelling Topical Group, and ITPA Pedestal and Edge Topical Group, *Nucl. Fusion* **47**, S18 (2007).

<sup>7</sup>X. Garbet, P. Mantica, C. Angioni, E. Asp, Y. Baranov, C. Bourdelle, R.

Budny, F. Crisanti, G. Cordey, L. Garzotti, N. Kirneva, D. Hogewei, T. Hoang, F. Imbeaux, E. Joffrin, X. Litaudon, A. Manini, D. C. McDonald, H. Nordman, V. Parail, A. Peeters, F. Ryter, C. Sozzi, M. Valovic, T. Tala, A. Thyagaraja, I. Voitsekhovitch, J. Weiland, H. Weisen, and A. Zabolotsky, and the JET EFDA Contributors, *Plasma Phys. Controlled Fusion* **46**, B557 (2004).

<sup>8</sup>D. J. Applegate, C. M. Roach, S. C. Cowley, W. D. Dorland, N. Joiner, R. J. Akers, N. J. Conway, A. R. Field, A. Patel, M. Valovic, and M. J. Walsh, *Phys. Plasmas* **11**, 5085 (2004).

<sup>9</sup>M. H. Redi, W. Dorland, C. L. Flore, J. A. Baumgaertel, E. M. Belli, T. S. Hahm, G. W. Hammelt, and G. Rewoldt, *Phys. Plasmas* **12**, 072519 (2005).

<sup>10</sup>J. A. Wesson, *Tokamaks* (Oxford University Press, New York, 1997), Chaps. 2 and 8.

<sup>11</sup>G. Rewoldt, W. M. Tang, and M. S. Chance, *Phys. Fluids* **25**, 480 (1982).

<sup>12</sup>W. Dorland, F. Jenko, M. Kotschenreuther, and B. N. Rogers, *Phys. Rev. Lett.* **85**, 5579 (2000).

<sup>13</sup>Y. C. Lee, J. Q. Dong, P. N. Guzdar, and C. S. Liu, *Phys. Fluids* **30**, 1331 (1987).

<sup>14</sup>P. N. Guzdar, C. S. Liu, J. Q. Dong, and Y. C. Lee, *Phys. Rev. Lett.* **57**, 2818 (1986).

<sup>15</sup>W. Horton, B. G. Hong, and W. M. Tang, *Phys. Fluids* **31**, 2971 (1988).

<sup>16</sup>J. Q. Dong, W. Horton, and J. Y. Kim, *Phys. Fluids B* **4**, 1867 (1992).

<sup>17</sup>J. W. Connor and R. J. Hastie, *Plasma Phys. Controlled Fusion* **46**, 1501 (2004).

<sup>18</sup>A. Fivaz, T. M. Tran, K. Appert, J. Vaclavik, and S. E. Parker, *Phys. Rev. Lett.* **78**, 3471 (1997).

<sup>19</sup>G. L. Falchetto and M. Ottaviani, *Phys. Rev. Lett.* **92**, 025002 (2004).

<sup>20</sup>T. H. Watanabe, H. Sugama, and S. Ferrando-Margalet, *Phys. Rev. Lett.* **100**, 195002 (2008).

<sup>21</sup>Z. Lin, T. S. Hahm, W. W. Lee, W. M. Tang, and R. B. White, *Science* **281**, 1835 (1998).

<sup>22</sup>B. Jhowry and J. Anderson, *Phys. Plasmas* **10**, 782 (2003).

<sup>23</sup>V. G. Panchenko, V. N. Pavlenko, E. Naslund, and L. Stenflo, *Phys. Scr.* **31**, 594 (1985).

<sup>24</sup>P. T. Bonoli, J. Ko, R. Parker, A. E. Schmidt, G. Wallace, J. C. Wright, C. L. Fiore, A. E. Hubbard, J. Irby, E. Marmor, M. Porkolab, D. Terry, S. M. Wolfe, and S. J. Wukitch, the Alcator C-Mod Team, J. R. Wilson, S. Scott, E. Valeo, C. K. Phillips, and R. W. Harvey, *Phys. Plasmas* **15**, 056117 (2008).

<sup>25</sup>C. S. Liu and V. K. Tripathi, V. S. Chan, and V. Stefan, *Phys. Fluids* **27**, 1709 (1984).